Received: 10 February 2024 | Revised: 29 April 2024 | Accepted: 3 May 2024

DOI: 10.1002/jbio.202400046

RESEARCH ARTICLE

JOURNAL OF BIOPHOTONICS

Selective induction of senescence in cancer cells through near-infrared light treatment via mitochondrial modulation

I. Kalampouka[1] | **R. R. Mould**[1] | **S. W. Botchway**[2] | **A. M. Mackenzie**[2] | **A. V. Nunn**[1,3] | **E. L. Thomas**[1] | **J. D. Bell**[1]

[1]Research Centre for Optimal Health, School of Life Sciences, University of Westminster, London, UK

[2]Research Complex at Harwell & Central Laser Facility, Rutherford Appleton Laboratory, Didcot, UK

[3]The Guy Foundation – The Guy Foundation Family Trust, Beaminster, UK

Correspondence
I. Kalampouka, Research Centre for Optimal Health, School of Life Sciences, University of Westminster, London, UK.
Email: i.kalampouka1@westminster.ac.uk

Funding information
The Guy Foundation Family Trust

Abstract

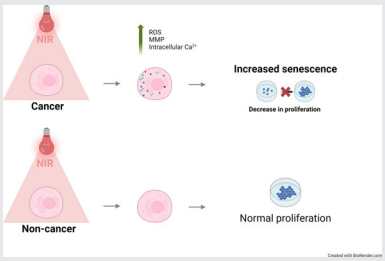

Photobiomodulation, utilising non-ionising light in the visible and near-infrared (NIR) spectrum, has been suggested as a potential method for enhancing tissue repair, reducing inflammation and possibly mitigating cancer-therapy-associated side effects. NIR light is suggested to be absorbed intracellularly, mainly by chromophores within the mitochondria. This study examines the impact of 734 nm NIR light on cellular senescence. Cancer (MCF7 and A549) and non-cancer (MCF10A and IMR-90) cell populations were subjected to 63 mJ/cm^2 NIR-light exposure for 6 days. Senescence levels were quantified by measuring active senescence-associated beta-galactosidase. Exposure to NIR light significantly increases senescence levels in cancer (10.0%–203.2%) but not in non-cancer cells ($p > 0.05$). Changes in senescence were associated with significant modulation of mitochondrial homeostasis, including increased levels of reactive oxygen species ($p < 0.05$) and mitochondrial membrane potential ($p < 0.05$) post-NIR-light treatment. These results suggest that NIR light modulates cellular chemistry, arresting the proliferation of cancer cells via senescence induction while sparing non-cancer cells.

KEYWORDS
cancer, mitochondria, near-infrared light, photobiomodulation, ROS, senescence

1 | INTRODUCTION

Photobiomodulation (PBM) is the term used to describe the changes in cellular activity and transformation that occur in response to irradiation with extrinsic light under certain conditions [1]. The modern term PBM therapy (formerly known as low-level laser therapy), introduced by Mester in 1967, is a non-thermal use of light that is distinguished from daylight and other light-based therapies that rely on thermal effects [2].

PBM therapy traditionally utilises red to infrared light (600–1000 nm) to promote wound healing, reduce inflammation and manage pain and age-related symptoms [3–5]. PBM therapy has become increasingly popular due to its non-invasiveness and the ability of red to NIR light to reach deeper into human tissue (650 and

750 nm, respectively) compared to other wavelengths of light [6]. PBM technology is rapidly expanding, and the reduction of inflammation is considered one of the most widely accepted effects of PBM therapy [4, 7]. PBM can significantly reduce the expression of inflammatory marker genes in cells [8, 9], in whole tissues such as skin [10], and in experimental ageing models such as age-related macular degeneration models [11]. The beneficial effects of PBM have also been observed in the treatment of diabetes [12], neural diseases and injuries, such as brain injuries [13–17] and alopecia [18]. Of particular interest is a review by Hamblin, Nelson and Strahan [19], which outlines the potential benefits of PBM for cancer patients, including the management of cancer-treatment side effects and the direct, selective targeting of cancer cells and tumours. Moreover, near-infrared photoimmunotherapy (NIR-PIT), which is an anti-cancer NIR-activated immune response, is undergoing Phase 3 clinical trials, specifically targeting localised advanced cancer [20]. In addition, clinical trials have shown increased survival in cancer patients receiving PBM, suggesting its potential as a supportive therapy to complement NIR-PIT [21].

Mechanistically, PBM occurs when cells absorb sufficient energy from photons to induce a state change in function. To facilitate this process, the cell must contain a molecule or a part thereof, referred to as a chromophore, possessing electrons in a low-energy orbit, possibly vibrionic transition, that can be excited by photons to transition to a higher energy orbit [22]. Karu identified cytochrome c oxidase (CCO) in the mitochondrial respiratory chain as one of the primary cellular chromophores essential for PBM, and subsequently suggested the use of retrograde mitochondrial signalling to explain how a short exposure to light could result in long-lasting effects on the organism, spanning from hours to even weeks [23].

Located in Complex IV within the mitochondria respiratory chain, CCO is the terminal enzyme in mitochondrial oxidative phosphorylation (OXPHOS) and is responsible for catalysing the reduction of oxygen to produce energy for cellular metabolism in the form of adenosine triphosphate (ATP) [5, 13, 24]. The level of metabolic energy generated via mitochondrial oxidative phosphorylation is directly related to the activity of CCO; as CCO activity increases, so does oxygen consumption and energy production [17]. Since Karu's work, several studies have observed changes in CCO activity following PBM [5, 25]; however, others have shown that PBM-induced cellular changes do not necessitate CCO involvement [26].

There are several suggested pathways by which PBM can retrograde mitochondrial signalling and enhance cellular function. The first involves the absorption of photons by CCO, which leads to the release of inhibitory nitric oxide (NO) and change of reactive oxygen species (ROS) levels and, in turn, increases OXPHOS and mitochondrial membrane potential (MMP) [23]. The second pathway involves ion channels sensitive to photonic stimulation, which can allow an increased number of calcium ions (Ca^{2+}) to pass through the cellular membrane [3, 4]. Alternative mechanisms include potentially modulating water order around the mitochondria [27].

Activation of these potential chromophores can change the ultrastructure and dynamics of mitochondria, resulting in a further increase of mitochondrial Ca^{2+}, ROS, ATP production and various other signalling molecules, which can activate different transcription factors in the nucleus through mitochondria-nucleus communication [3, 14, 15]. These transcription factors can, in turn, activate gene expression affecting cell survival, such as cell migration and proliferation, wound healing, anti-inflammatory signalling and protein synthesis [3, 15, 28, 29].

In addition to its role in cellular metabolism and energy production, mitochondria also play a crucial role in cellular responses to stress. One such cellular response is senescence—this is an intermediate stress response that occurs when the stressor is not damaging enough to induce apoptosis or the cell is unable to ensure homeostasis after exposure to the stressor [30, 31]. The senescent cell is a highly metabolically active system that has permanently lost its ability to proliferate [32, 33]. Furthermore, senescence is a multi-step process that can be initiated via either cells reaching their Hayflick limit (replicative senescence; [32]), or via diverse stressors, including oxidative damage and chemotherapeutic drugs [34].

Besides senescence's role as a cell-autonomous tumour suppression mechanism, the effect of cellular senescence is beneficial to many physiological processes, including normal development and tissue remodelling [35], wound healing [36, 37] and tissue repair [38, 39]. Senescence is an example of antagonistic pleiotropy [40–42], where younger organisms increase their health and survival rate, whereas, as they age, they experience adverse effects from senescence, including disruption of homeostasis, increased inflammation and the onset of diseases [43–45].

In the investigation of the beneficial outcomes associated with PBM, it is relevant to highlight resemblances between these effects and those observed in senescence, including wound healing [36, 37] and tissue repair [38, 39]. Thus, this research aims to investigate the potential interaction between NIR light and the induction of senescence. Given that senescence can both affect and be affected by levels of ROS, and PBM can affect ROS signalling in the cells [46], we hypothesise that NIR treatment may increase senescence.

2 | RESULTS

2.1 | Doxorubicin induces senescence in cancer and non-cancer cell lines

Following treatment with 0.25 μM Dox, MCF7 breast cancer cells ($N = 8$), MCF10A breast non-cancer cells ($N = 7$), A549 lung cancer cells ($N = 9$) and IMR-90 lung fibroblasts ($N = 4$) exhibited a significant increase in fluorescence of the CellEvent Green Senescent Assay. This is indicative of a significant increase in senescence: 53.76% ± 7.5 ($p \leq 0.001$), 101% ± 9.7 ($p < 0.0001$), 179% ± 30 ($p < 0.0001$) and 55% ± 8.2 ($p \leq 0.001$), respectively (Figure 1).

2.2 | Potential thermal effects post-NIR-light exposure

The maximum wavelength of the light-emitting diode (LED) used in this study was characterised at 734 nm (Figure 2A). Using a FireSting sensor that is sensitive to

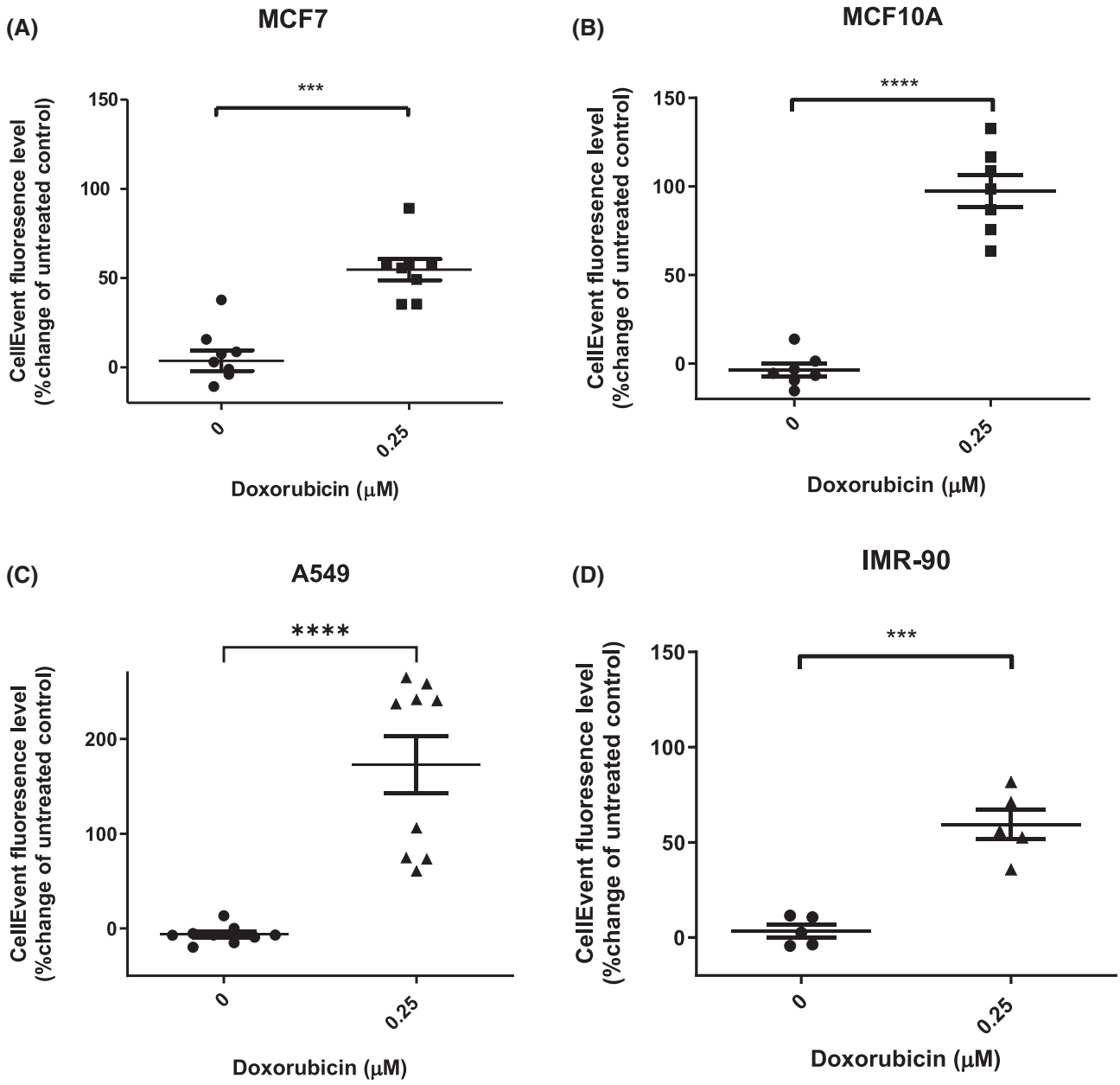

FIGURE 1 The effect of Dox on cellular senescence induction: (A) MCF7 ($N = 8$), (B) MCF10A ($N = 7$), (C) A549 ($N = 9$) and (D) IMR-90 ($N = 4$) cells were treated with 0.25 μM Dox. Senescent levels were quantified with CellEvent Green Senescent fluorescence intensity. Data are presented as mean changes in median fluorescent intensity compared with vehicle control ± SEM. ***$p \leq 0.001$; ****$p \leq 0.0001$.

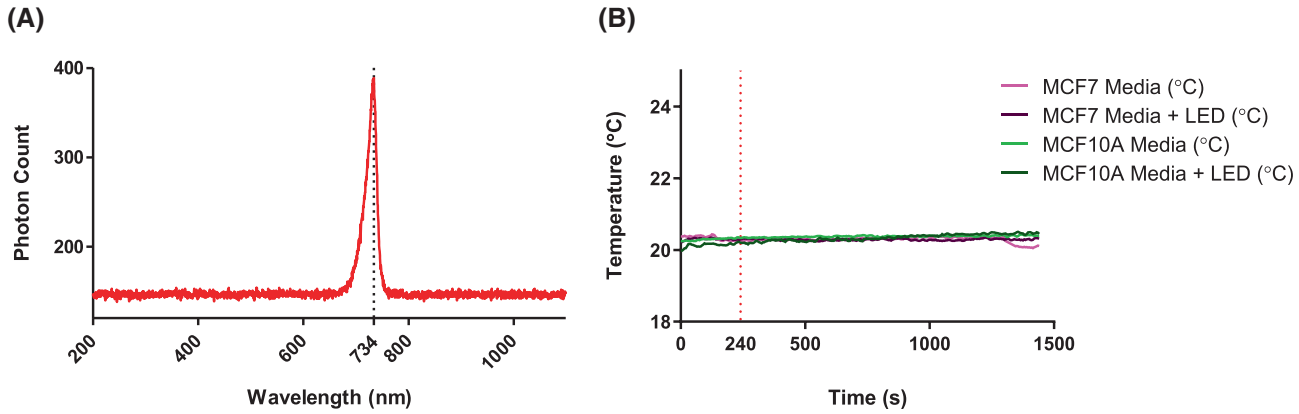

FIGURE 2 LED light characterisation. (A) The wavelength of LED light determined using a spectrometer. The emission peak was determined to be 734 nm. (B) No thermal effect of LED light on cancer and non-cancer cell media. The LED light was on between 240 and 1440 s.

temperature changes, no thermal changes were observed in the media during and post-NIR-light exposure (Figure 2B).

2.3 | NIR light increases senescence in cancer cellular populations

NIR-light treatment induces senescence in MCF7 and A549 cancer cells in the absence of Dox. Additionally, NIR-light treatment increases senescence in Dox-induced senescent populations of the same cell lines. In more detail, upon 6-days exposure of MCF7 and A549 to 63 mJ/cm^2 NIR-light irradiation, increased senescence was observed: MCF7 ($N = 6$) 10.0% ± 5.4 in untreated cells and 13.7% ± 6.0 in 0.25 μM Dox treated cells; A549 ($N = 6$): 14.5% ± 5.5 in untreated cells and 203.2% ± 63.2 in 0.25 μM Dox treated cells. In contrast, non-cancer MCF10A cells ($N = 6$) and IMR-90 fibroblasts ($N = 3$) remained unaffected. Significant interactions between Dox and NIR-light treatments were observed only in the A549 cell line among the four tested (NIR light–Dox interaction; MCF7: $p = 0.651$, A549: $p = 0.008$; MCF10A: $p = 0.919$, IMR-90: $p = 0.542$; Figure 3).

2.4 | NIR-light treatment regulates ROS in cancer cells

As expected, Dox-inducted senescence led to a significant increase in ROS levels in both cancer and non-cancer cells: MCF7 ($N = 7$): 130.2% ± 22.5, $p < 0.0001$; MCF10A ($N = 9$): 135.8% ± 37.9, $p < 0.0001$. NIR-light treatment led to a significant increase in ROS levels in both control (absence of Dox; 36% ± 11.3 increase) and senescent (Dox-treated; 53.9% ± 37.5 increase) MCF7 cancer cells ($N = 7$; $p = 0.015$; Figure 4A) but not in non-cancer MCF10A cells ($N = 8$; $p = 0.935$; Figure 4B). No Dox–NIR-light significant interaction was observed in terms of ROS levels ($p = 0.250$).

2.5 | NIR-light treatment affects mitochondrial membrane potential and intracellular Ca^{2+} levels in MCF7 cancer cells

Having observed the changes in ROS levels induced by NIR-light treatment in MCF7 cancer cells, we examined the potential effects of NIR light on another indicator of mitochondrial function, Ca^{2+}. As expected, both intracellular ($N = 8$; $p < 0.0001$) and mitochondrial ($N = 6$; $p < 0.0001$) Ca^{2+} levels were significantly increased in Dox-induced senescence, as determined by flow cytometry of Fluo-4 and Rhod2 fluorescence intensity (Figure 5A,B). Post-NIR-light treatment, no changes in mitochondrial Ca^{2+} levels were observed ($N = 6$; $p = 0.601$), whereas intracellular Ca^{2+} levels were significantly increased in both control (absence of Dox; 13.9% ± 6.4 increase) and senescent (Dox-treated; 39.4% ± 24.1 increase) MCF7 cancer cells ($N = 6$; $p = 0.037$). No Dox–NIR-light significant interactions were observed in terms of intracellular Ca^{2+} levels ($p = 0.302$).

Although no significant changes in MMP were observed in Dox-induced senescent MCF7 cells ($N = 7$; $p = 0.421$; Figure 5C), NIR-light treatment led to a significant increase in MMP, both in control (absence of Dox; 13.0% ± 4.0 increase) and senescent (Dox-treated; 7.1% ± 6.3 increase) MCF7 cancer cells ($N = 7$; $p = 0.012$). No Dox–NIR-light significant interactions were observed in terms of MMP ($p = 0.428$).

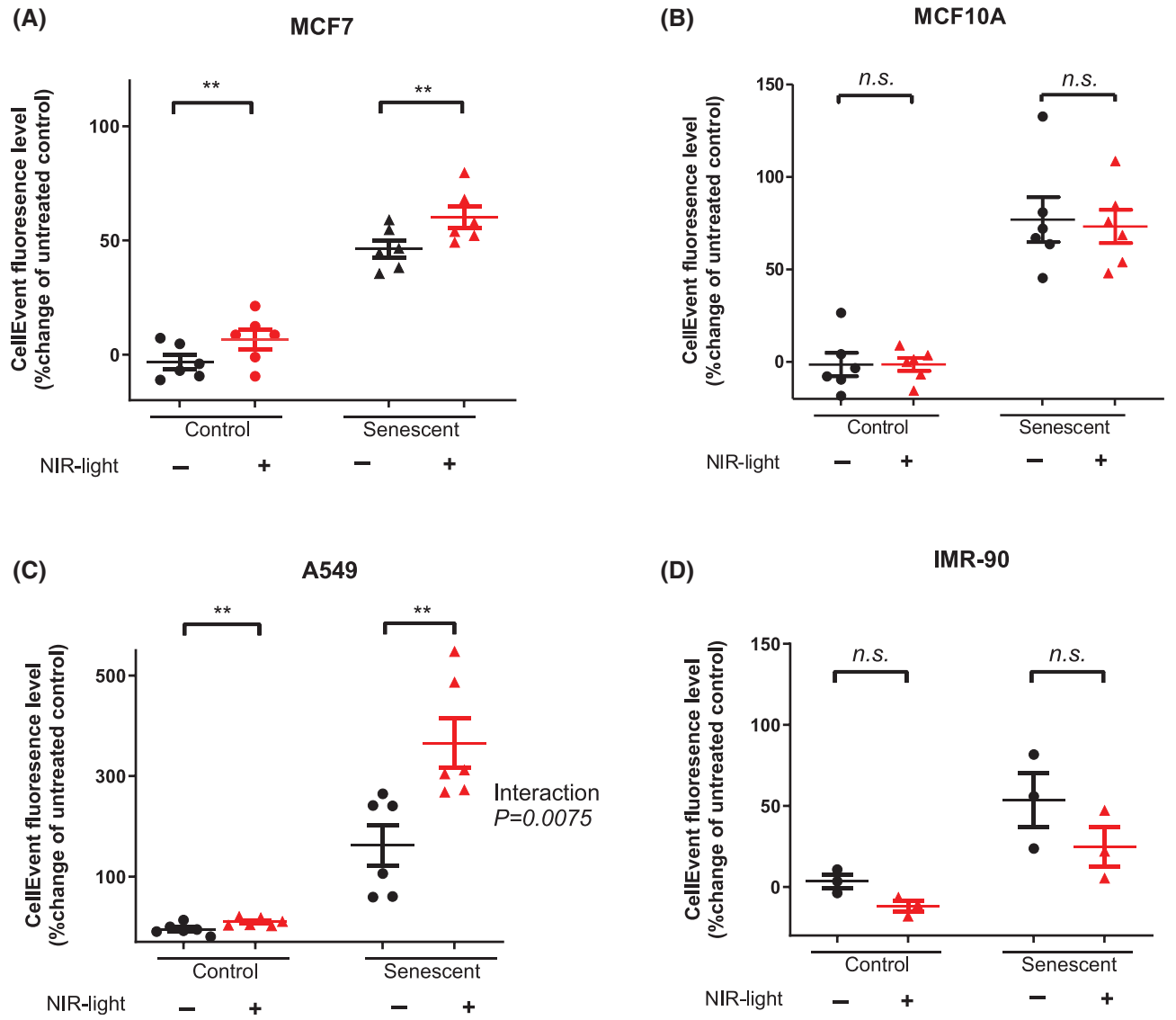

FIGURE 3 The effect of near-infrared (NIR) light on control and senescent cells measured by flow cytometry. (A) MCF7 ($N = 6$), (B) MCF10A ($N = 6$), (C) A549 ($N = 6$) and IMR-90 ($N = 3$) control (absence of Dox) or senescent (Dox-treated) populations were either exposed to NIR light or left untreated. Senescent levels were quantified with CellEvent Green Senescent fluorescence intensity. Data are presented as mean changes in median fluorescent intensity compared with an untreated control ± SEM. $^{**}p \leq 0.01$, n.s., non-significant ($p > 0.05$).

3 | DISCUSSION

3.1 | Dox-induced senescence as a standard protocol for four different cellular models

In this study, we applied a Dox-based senescence induction protocol to four different mammalian cell lines, including both cancerous and non-cancerous cells, which was detected and quantified using the same single assay (CellEvent Senescence Green Flow Cytometry Assay). The Dox-based method was chosen as it is now well established, inducing significant senescent populations in different cell lines [47, 48], This method was further validated in the present study using flow cytometry analysis, which demonstrated positive staining results with a fluorescence dye for SA β-gal activity, a distinctive feature of senescence, in all four cell populations. An advantage of the SA β-gal assay is its ability to distinguish senescence from quiescence, as only the former exhibits increased lysosomal content and β-gal enzymatic activity [49]. Senescent cells also display an increase in both lysosome number and size, leading to an expansion of the lysosomal compartment and lysosome biogenesis [50–52]. Thus, our results indicate non-reversible proliferation arrest on cellular populations.

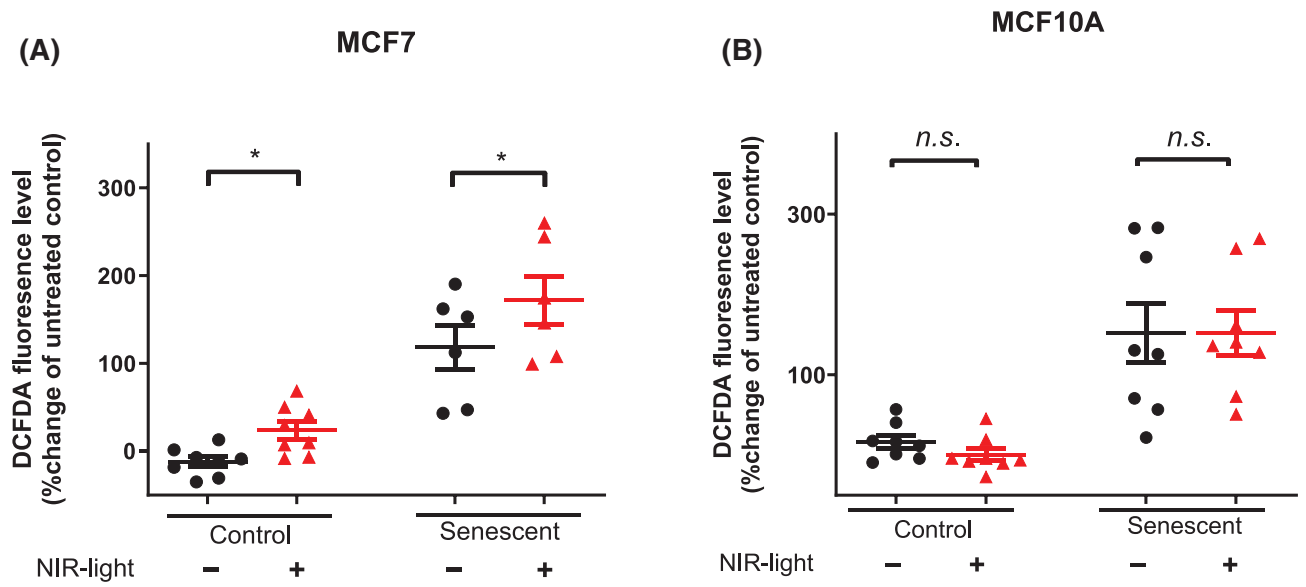

FIGURE 4 The effect of near-infrared (NIR) light on reactive oxygen species (ROS) levels measured by flow cytometry. (A) MCF7 ($N = 7$) and (B) MCF10A ($N = 9$) control (absence of Dox) or senescent (Dox-treated) populations were either exposed to NIR light or left untreated. ROS levels were quantified with DCFDA fluorescence intensity. Data are presented as mean changes in median fluorescent intensity compared with an untreated control ± SEM. *$p \leq 0.05$, n.s., non-significant ($p > 0.05$).

3.2 | NIR-light treatment increases senescence in cancer cells

Using the senescence induction protocols described above, we show that NIR-light treatment (734 nm; fluence = 63 mJ/cm^2) can lead to significant induction of senescence in cancer cell lines while sparing non-cancer cells. Indeed, exposure to NIR light induced senescence in cancer cells in the absence of Dox treatment, as well as increased the effect of Dox-induced senescence in these cell lines. Moreover, NIR-light treatment exhibited a significant detectable interaction with Dox, leading to an enhanced increase in senescence within the lung cancer A549 model. Since senescence is a permanent cell cycle arrest, this reflects a significant decrease in the number of cells. Previous studies have evaluated PBM therapy on cancer cell proliferation but failed to test for senescence. For instance, Hu et al. showed that A2058 melanoma cell lines increased in number in response to PBM (632.8 nm light) but used higher fluences (intensity): 500, 1000 and 2000 mJ/cm^2. The same dose–response increase was observed in CCO activity of this cell line [53]. Magrini et al. reported similar results, who tested different fluences (5, 28.8 and 1000 mJ/cm^2) of 633 nm light treatment on MCF7 breast cancer cells [54]. Cell number increased together with metabolic activity at a 1000 mJ/cm^2 fluence, whereas no increase in cell number or metabolic activity was reported at a fluence of 5 mJ/cm^2. In the present study, though the light characteristic was similar (734 nm) to those used by Hu et al and Magrini et al, its fluence was lower (63 mJ/cm^2), which may explain the differential effect of our treatment. Interestingly, when the light treatment used by Magrini et al. decreased to a fluence range (28 mJ/cm2) similar to that used in our study, they observed no increase in cell population, but higher metabolic activity compared with cells treated with light of 5 mJ/cm^2 [54]. This would suggest that they may be inducing senescence in their cell populations but was not tested for in that particular study.

Our results, together with those previously published, suggest that NIR-light senescence induction in cancer cells, but not normal cells, may display a biphasic effect, with a fluence 'sweet-spot' above 20 mJ/cm^2 and below 300 mJ/cm^2, [54] at wavelengths of 600–800 nm [3–5]. However, when the fluence is increased above this range, NIR treatment can lead to an increase in cellular proliferation and metabolic rates in cancer cells. The overall mechanism by which this may occur remains unknown and requires further investigation.

It is well-established that the effectiveness of PBM on a particular target tissue can depend on various factors, including the light source, wavelength, energy density, light pulse structure, and duration of the light application. These parameters play a significant role in determining the optimal treatment outcomes [55]. A biphasic dose–response curve, also known as hormesis, illustrates that excessively low or high doses such as fluence (mJ/cm^2), irradiance (mW/cm^2), duration of application, or treatment design may result in no

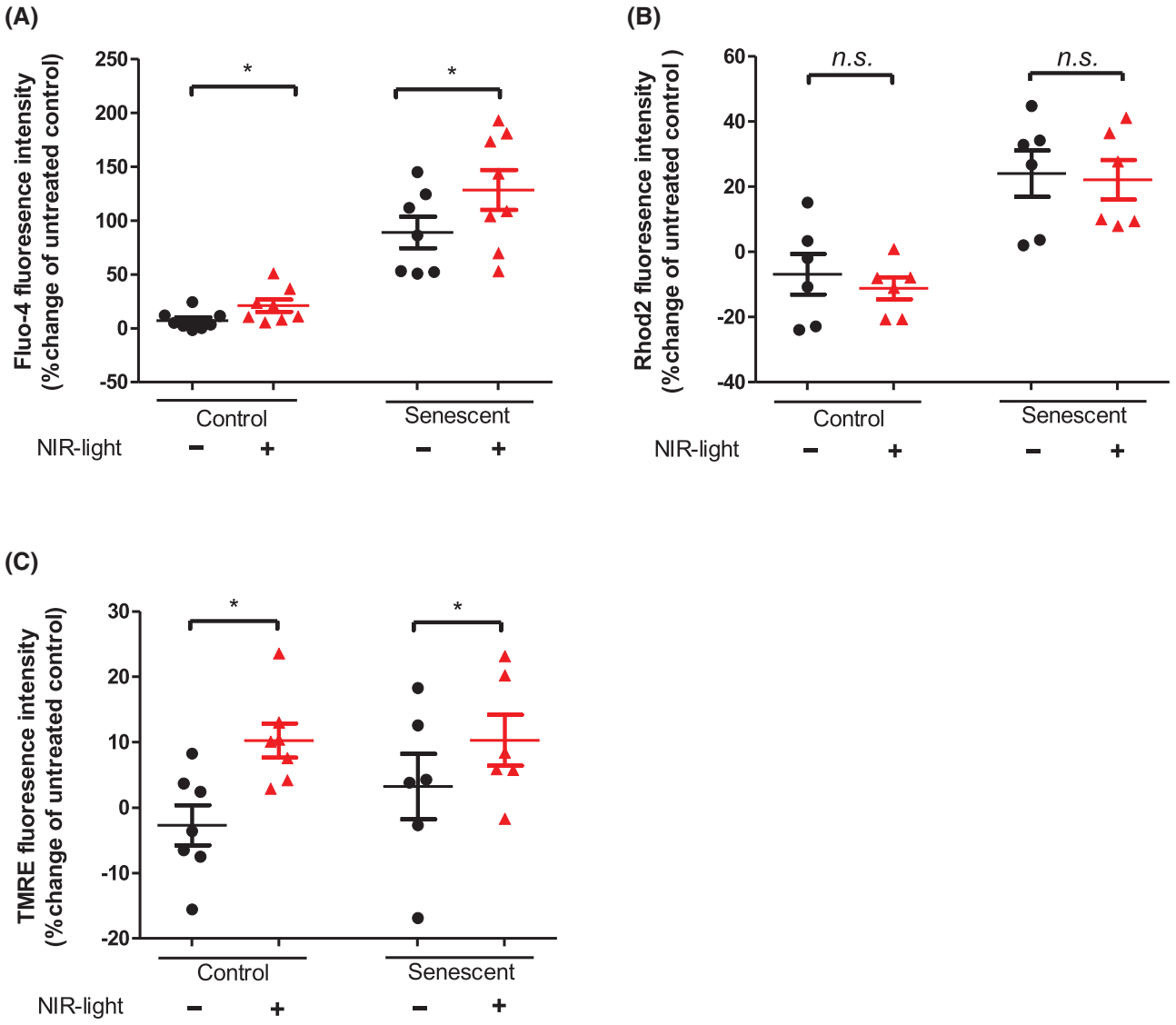

FIGURE 5 The effect of near-infrared (NIR) light on MCF7 homeostasis and cellular function. MCF7 control (absence of Dox) or senescent (Dox-treated) populations were either exposed to NIR light or left untreated. (A) Intracellular Ca^{2+} levels were quantified with Fluo-4 fluorescence intensity ($N = 8$); (B) mitochondrial Ca^{2+} levels were quantified with Rhod2 fluorescence intensity ($N = 6$); (C) mitochondrial membrane potential (MMP) was quantified with tetramethylrhodamine ethyl ester (TMRE) fluorescence intensity ($N = 7$). All tests were measured with flow cytometry. Data are presented as mean changes in median fluorescent intensity compared with an untreated control ± SEM. *$p \leq 0.05$, n.s., non-significant ($p > 0.05$).

significant effect or opposite inhibitory effects [55, 56]. Thus, it is likely that NIR-light treatment may be hormetic in nature, with cancer cell proliferation increasing at very low/high light fluence but inducing senescence at a specific range.

3.3 | NIR light does not induce senescence in non-cancer cell lines

In the current study, we observed that while cancer cells showed a significant permanent cell cycle arrest following NIR-light treatment, non-cancer cells remained unaffected. However, previous studies have reported that PBM treatment at doses of over 1000 mJ/cm^2 can significantly increase the proliferation of healthy cell lines, including stem cells derived from human exfoliated deciduous teeth [57], human osteoblast-like cells [58], melanocytes [59], human adipose stem cells [60] and skin fibroblasts WS1 [61]. Similar effects have also been reported in healthy human umbilical cord blood-derived mesenchymal stem cells [62] and healthy canine epidermal keratinocyte progenitors [63] following PBM treatment with fluence

ranges of 300–100 mJ/cm^2, the latter fluence being closer to our NIR-light characteristic. At present, it is unclear why there is a discrepancy between the results of the current study and those reported in the literature, but it indicates that the response of non-cancer cells to PBM may be related to tissue origin [64], with different cell type showing differential activation 'sweet-spots'.

3.4 | NIR-light treatment increases ROS levels in cancer MCF7 but not in non-cancer MCF10A cells

It has been previously suggested that modulation of ROS levels is one of the primary effects of PBM [65]. We, therefore, hypothesised that increasing intracellular ROS with NIR light should lead to senescence induction in cancer cells, since their metabolism is more complex than normal cells and are able to switch readily between glycolosis and oxidative phosphorelation [66]. The results from our study appear to confirm this, as the observed increase in senescence in cancer cells was accompanied by significant increases in ROS levels, as well as alteration in MMP and Ca^{2+} levels.

It is well described that redox plays a key role in the cell cycle, controlling cell growth, proliferation and death [67]. It is therefore of no surprise that cellular senescence involves nuclear factor kappa B (NF-kB) activation [68, 69] with mitochondria and ROS being known drivers of senescence, both in vivo and in vitro [70–72]. ROS appears to play a reciprocal role in cellular senescence, as the process leads to an increase in ROS, which in turn can induce senescence [71]. It is also well-established that ROS can activate transcription factors such as NF-kB [73, 74]. This nuclear transcription factor is known to play a critical role in inflammation, cell proliferation and survival, and is known to regulate the expression of more than a 100 genes, including those that promote antioxidant, anti-apoptotic, pro-proliferation and pro-migration functions [46]. Magrini et al had previously proposed that ROS production, after PBM treatment, alters cellular metabolism via interactions with nuclear transcription factors such as NF-kB [54]. This was subsequently confirmed by Hamblin who showed that a burst of ROS could activate the NF-kB signalling pathway following PBM treatment [46]. This would suggest that the observed increase in senescence in cancer cells, but not in non-cancer cells, in the current study, was a direct consequence of the elevation in ROS production associated with PBM, which in turn would lead to NF-kB signalling pathway activation and thus senescence.

3.5 | NIR light changes MCF7 cancer cell homeostasis and mitochondrial dynamics, altering intracellular Ca^{2+} levels and MMP

It has been previously suggested that retrograde signalling arising from the initial photoreceptors in the mitochondria can be mediated by ROS, MMP and altered Ca^{2+} levels [75]. In the current study, we confirm that ROS, MMP and intracellular Ca^{2+} levels show significant changes after NIR-light treatment.

MMP increased in cancer cells after NIR-light treatment. It is generally accepted that ROS production and MMP are highly correlated [76]. Indeed, as suggested by Aon and colleagues in their redox-optimised ROS balance hypothesis, mitochondria evolved to maximise energy output while keeping ROS production to a minimum by operating at an intermediate redox state, where electron flow and anti-oxidant balance systems are key. This hypothesis explains why either an increase in MMP, for example due to hypoxia, or a decrease, for example due to excessive uncoupling, both give rise to ROS [77]. Korshunov et al., using isolated mitochondria from rat cardiac muscle, showed that even a slight increase in MMP was sufficient to produce H_2O_2 in mitochondria [78]. Hence, PBM may induce a rise in the MMP due to an increase in electron transport chain, which can result in increased ROS levels [15, 76]. Additionally, decreasing MMP is correlated with mitochondrial dysfunction and increased ROS production, which are both key signals for mitochondrial turnover, but can contribute to tissue damage [15]. This suggests that senescence induction after NIR exposure is the result of ROS as a secondary messenger and not general mitochondrial dysfunction.

Although no change in mitochondrial Ca^{2+} levels was recorded in this study, there was a significant increase in intracellular Ca^{2+} levels post-NIR-light exposure. PBM and the use of non-thermal NIR light notably influence intracellular Ca^{2+} levels, as demonstrated across various studies, including cervical cancer HeLa cells [79], neuroblastoma, neuron cells [80] and osteoblasts [81]. Studies by Amaroli et al. [65] demonstrate that specific wavelengths and energies of light impact calcium influx, either directly or by affecting mitochondrial activity. The interplay between ROS and Ca^{2+} signalling, as highlighted by Görlach et al., suggests a bidirectional relationship, where oxidative stress triggers calcium influx from different cell sources, while Ca^{2+} can increase ROS production [82]. Finally, as Ca^{2+} serves as a critical cellular secondary messenger [83], changes in Ca^{2+} levels induced by NIR light may regulate senescence in cancer cells. As mitochondria are central to calcium signalling [84], it is surprising that we did not see any changes in mitochondrial calcium, however, it is

entirely possible that the effects were too small to measure or occurred very quickly. Calcium influx into mitochondria would stimulate their activity, potentially raising their MMP, but the flow of calcium in and out of the mitochondrion is very tightly controlled. Thus, further research is required to understand their precise role in the observed shifts in intracellular calcium.

3.6 | Explaining the differential response of cancerous and non-cancerous cells to PBM

Our results clearly demonstrate that the potential differences between cancerous and non-cancerous cells are associated with mitochondria and ROS. Warburg was the first to describe what is now known as the 'Warburg effect'—the phenomenon whereby cancer cells, despite the presence of oxygen, seems to rely on glycolysis, so-called 'aerobic glycolysis', instead of OXPHOS [85, 86]. A recent study revealed that defects in CCO can cause a metabolic shift to glycolysis (Warburg effect induction) and promote cancer progression. The loss of CCO activity results in the activation of several oncogenic signalling pathways and the upregulation of genes involved in cell signalling, cell migration and extracellular matrix interactions [87]. Since CCO has previously been suggested as containing chromophores that could be responsible for PBM, it explains why cancer cells and normal cells might exhibit varied responses to PBM [19]; PBM can increase energy demand in cancer cells, increase metabolism and increase ROS activity that activates transcription factors. On the other hand, in healthy cells, PBM may induce a small burst of ROS that triggers protective mechanisms and minimises damage, placing the cell in a position that overcomes stress and escapes senescence induction.

In parallel, during senescence, the amount of ATP produced by mitochondria decreases, and more ATP is produced through glycolysis. This compensatory response to mitochondrial dysfunction due to senescence results in an increase in mitochondrial abundance and a shift towards glycolytic ATP production [88]. In a study using alpha mouse liver 12 (AML12) cells, the senescent population had greater glycolytic potential, together with increased mitochondrial activity and damage due to proton leak—this did not increase ATP production despite the increased mitochondrial activity in senescent cells [89]. Interestingly, a study that investigated the metabolic effects of acute 780 nm LED light of 5 J/cm^2 on healthy human dermal fibroblasts neonatal (HDFn) and squamous carcinoma (SCC-25) cells demonstrated that the cancer cells were more glycolytic. After 0 and 4 h of treatment, the cancer cells showed increased ROS production and ATP levels, whereas the healthy cells did not; while 24 h post-treatment, healthy cells increased proliferation, whereas cancer cells did not [90]. This suggests that the initial ROS increase, together with the increase in metabolic demand, might play a role in decreased proliferation rates in comparison with healthy cells.

4 | CONCLUSION

The current study demonstrates that NIR light inhibits proliferation in cancer cells (MCF7 and A549) but not in non-cancer cell lines (MCF10A and IMR-90). The proposed general mechanism, partially detailed in the literature of PBM action, appears to involve an increase of ROS production [91, 92], which our data seem to confirm, and thus, could be operative in this senescence mode. This mechanism takes into consideration the Warburg effect, where cancer cells have a greater shift towards glycolysis, leading to increased ROS levels. The combination of the already elevated ROS levels in cancer cells and PBM-induced ROS increase activates a signal cascade towards senescence and permanent cell cycle arrest as a stress response. This mitochondrial/ROS-based mechanism would support the well-described anti-inflammatory and wound-healing properties observed with PBM. Future work is needed to establish the optimal fluence and wavelength for PBM and determine its potential as a cancer-selective therapy, as well as the relationship to calcium signalling and the precise location of ROS production.

5 | METHODS

5.1 | Cell lines

Human breast cell line *MCF10A* was grown in Dulbecco's modified eagle medium (DMEM): F12 (Life Sciences, UK), supplemented with 5% horse serum (Thermo Fisher, UK), 2% penicillin/streptomycin, 20 ng/mL epidermal growth factor (Merck, UK), 0.5 mg/mL hydrocortisone (Merck, UK), 100 ng/mL cholera toxin (Merck, UK) and 10 μg/mL insulin (Merck, UK). Human breast adenocarcinoma cell line *MCF7* and human lung fibroblast cell line *IMR-90* purchased from American Type Culture Collection (ATCC) were grown in Eagle minimum essential medium (Thermo Fisher, UK), supplemented with 10% fetal bovine serum (FBS), 1% l-glutamine and 1% penicillin/streptomycin. Human lung

cancer cell line A549 purchased from ATCC was grown in DMEM high glucose (Thermo Fisher, UK), supplemented with 10% FBS and 1% penicillin/streptomycin.

5.2 | Treatment protocols for senescence induction

Premature cellular senescence was induced by treatment with 0.25 μM doxorubicin (Dox; Tocris, Bio-techne, Bristol) for 24 h and subsequently extended culture in drug-free media for a further 5 days [48]. Dox was dissolved in autoclaved deionised water to a stock concentration of 100 mM.

5.3 | NIR-light characterisation

LED NIR light exposure was achieved by using a premounted 7—LED array of NIR (734 nm) Rebel LEDs (Luxeon Star LED, Alberta, Canada) mounted on a SinkPAD-II 40 mm Round 7-Up base with a power output of between 0.328 and 0.420 mW (fluence = 63 mJ/cm^2, power density = 0.05 mW/cm^2), as described by [9].

LED light characterisation was performed at the Research Complex at Harwell Science & Technology Facilities Council. The wavelength range was measured using a portable USB high-resolution fibre optic HR2000CG UV-NIR spectrometer (Ocean Optics Inc., Florida, USA), and the output power was recorded on a PM100D power meter with an S120VC photodiode power sensor (Thorlabs Inc., New Jersey, USA). Temperature changes in media exposed to LED light were measured with a FireSting optical temperature sensor and recorded by an FSO_2 temperature meter (Pyroscience, Germany). The temperature sensor was positioned at the centre of the plate well containing cell-free media, and temperature readings were taken every 5 s over a total of 1440 s (24 min). The LED light was switched on at 240 s. Media for both cancer and non-cancer cell lines were utilised and compared against control media with no LED irradiation.

5.4 | NIR-light treatment

Briefly, 5×10^4 cells were seeded in two separate 6-well plates. One plate ('control') was left in the dark and the second ('treated') was exposed to 63 mJ/cm^2 NIR light. The light treatment consisted of exposure to NIR light for 20 min, every day, for 6 days. The LED array was placed 4 cm below the culture plate and in between two wells to illuminate the cells. The control population was covered and was not exposed to NIR light. Any other cell treatment (e.g., Dox treatment) was performed normally in the period of these 6 days, before the light treatment.

5.5 | Flow cytometry assay for senescence quantification

Flow cytometry was used for the quantification of senescent levels in cellular populations [93]. The CellEvent™ Senescence Green Flow Cytometry Assay Kit (Thermo Fisher, UK) was used for flow detection of cellular senescence using a fluorescent dye that binds to the senescence-associated beta-galactosidase (SA-beta-gal) enzyme, and the assay was performed according to manufacture protocol [94].

Flow cytometry measurements were performed with a BD LSRFortessa™ X-20 Analyser flow cytometer (BD Biosciences, New Jersey, USA), and data were recorded/analysed using BD FACSDiva™ Software. The AlexaFluor channel (488 nm laser) was used to capture the uptake of stained cells. For analysis, the cell population was selected on a forward/side scatter plot to exclude debris cellular aggregates, and 10 000 gated events were recorded. The median fluorescent intensity was recorded.

5.6 | Detection and quantification of ROS

The 2′,7′–dichlorofluorescin diacetate (DCFDA) stain was used to detect changes in the levels of ROS in live cells. After treatment, cells were washed with phosphate-buffered saline (PBS) and incubated with 30 μM DCFDA (Sigma, UK) at 37°C 5% CO_2 for 30 min, protected from light. DCFDA fluorescence was quantified by flow cytometry—the AlexaFluor channel (488-nm laser) was used to capture the uptake of stained cells.

5.7 | Assessment of mitochondria Ca^{2+} levels

The cell permeant Rhod-2 stain was used to label mitochondrial Ca^{2+} in live cells. After treatment, cells were incubated with 1 μM Rhod-2 (Thermo Fisher, UK) in Phenol Red Free media, at 37°C 5% CO_2 for 30 min, protected from light. Rhod-2 fluorescence signals were quantified by flow cytometry—the PE channel (575-nm laser) was used to capture the uptake of stained cells.

5.8 | Assessment of intracellular Ca^{2+} levels

The cell permeant Fluo-4 stain was used to label intracellular Ca^{2+} in live cells. After treatment, cells were incubated with 1 μM Fluo-4 (Thermo Fisher, UK) in Phenol Red Free media, at 37°C 5% CO_2 for 30 min, protected

from light. Fluo-4 fluorescence signals were quantified by flow cytometry—the PE channel (575-nm laser) was used to capture the uptake of stained cells.

5.9 | Assessment of MMP

The cell permeant tetramethylrhodamine ethyl ester (TMRE) stain was used to label active mitochondria in live cells. After treatment, cells were incubated with 500 nM TMRE (Sigma, UK) in Phenol Red Free media, at 37°C 5% CO_2 for 30 min, protected from light. Activated mitochondria sequester TMRE was quantified by flow cytometry—the PE channel (575-nm laser) was used to capture the uptake of stained cells.

5.10 | Statistical analysis

Results are expressed as the mean ± standard error of the mean. All data sets were tested for significant outliers (alpha = 0.05) via Grubbs' test.

For comparison between two groups, a two-tailed, unpaired *T*-test (*F*-test; *p*-value) was applied. The effect of NIR LED light treatment in control and senescent populations in senescence induction (CellEvent Senescent Green fluorescent assay), ROS levels (DCFDA fluorescent assay), mitochondrial Ca^{2+} levels (Rhod2 fluorescent assay) and intracellular Ca^{2+} levels (Fluo-4 fluorescent assay) were compared with a mixed-model two-way ANOVA, with Bonferroni post hoc testing performed where indicated. Statistical analyses were performed with GraphPad Prism (USA) version 10.0.2.

AUTHOR CONTRIBUTIONS

I. Kalampouka, R.R. Mould, A.V. Nunn, and J.D. Bell conceptualised the study. I. Kalampouka, R.R. Mould, S.W. Botchway, and A. Mackenzie conceived and performed experiments. I. Kalampouka and R.R. Mould analysed the data. I. Kalampouka, R.R. Mould, S.W. Botchway, A. Mackenzie, A.V. Nunn, E.L. Thomas, and J.D. Bell were involved in writing and had final approval of the manuscript.

ACKNOWLEDGMENTS

The LED light source was kindly gifted by Synlyte SAS, Massy Palaiseau, France.

FUNDING INFORMATION

This work was supported by The Guy Foundation Family Trust.

CONFLICT OF INTEREST STATEMENT

The authors declare that the research was conducted without any commercial or financial relationships that could be construed as a potential conflict of interest.

DATA AVAILABILITY STATEMENT

The raw data supporting the conclusions of this article will be made available by the authors, without undue reservation.

ORCID

I. Kalampouka https://orcid.org/0009-0005-0385-345X
R. R. Mould https://orcid.org/0000-0002-9353-1614
S. W. Botchway https://orcid.org/0000-0002-3268-9303
A. M. Mackenzie https://orcid.org/0000-0002-3308-6352
A. V. Nunn https://orcid.org/0000-0003-0728-1995
E. L. Thomas https://orcid.org/0000-0003-4235-4694
J. D. Bell https://orcid.org/0000-0003-3804-1281

REFERENCES

[1] S. Y. Tam, V. C. W. Tam, S. Ramkumar, M. L. Khaw, H. K. W. Law, S. W. Y. Lee, *Front. Oncol.* **2020**, *10*, 1255.
[2] E. Mester, G. Ludany, M. Selyei, B. Szende, G. J. Total, *Laser Rev.* **1968**, *1*, 3.
[3] L. F. de Freitas, M. R. Hamblin, *IEEE J. Sel. Top. Quantum Electron.* **2016**, *22*, 348.
[4] M. R. Hamblin, *AIMS Biophys.* **2017**, *4*, 337.
[5] X. Wang, F. Tian, S. S. Soni, F. Gonzalez-Lima, H. Liu, *Sci. Rep.* **2016**, *6*, 30540.
[6] C. Ash, M. Dubec, K. Donne, T. Bashford, *Lasers Med. Sci.* **2017**, *32*, 1909.
[7] F. Aimbire, R. Albertini, M. T. T. Pacheco, H. C. Castro-Faria-Neto, P. S. L. M. Leonardo, V. V. Iversen, R. A. B. Lopes-Martins, J. M. Bjordal, *Photomed. Laser Surg.* **2006**, *24*, 33.
[8] B. Aguida, M. Pooam, M. Ahmad, N. Jourdan, *Commun. Integr. Biol.* **2021**, *14*, 200.
[9] M. Pooam, B. Aguida, S. Drahy, N. Jourdan, M. Ahmad, *Commun. Integr. Biol.* **2021**, *14*, 66.
[10] M. Choi, S. Y. Na, S. Cho, J. H. Lee, *J. Korean Med. Sci.* **2011**, *26*, 454.
[11] R. Begum, M. B. Powner, N. Hudson, C. Hogg, G. Jeffery, *PLoS One* **2013**, *8*, e57828.
[12] P. M. Bodnar, A. O. Peshko, O. M. Prystupiuk, A. A. Voronko, D. V. Kyriienko, H. P. Mykhal'chyshyn, M. I. Naumova, *Lik. Sprava* **1999**, *6*, 125.
[13] F. d. S. Cardoso, D. W. Barrett, Z. Wade, S. Gomes da Silva, F. Gonzalez-Lima, *Front. Neurosci.* **2022**, *16*, 818005.
[14] A. S. C. Foo, T. W. Soong, T. T. Yeo, K.-L. Lim, *Front. Aging Neurosci.* **2020**, *12*, 89.
[15] M. R. Hamblin, *J. Neurosci. Res.* **2018**, *96*, 731.
[16] M. A. Naeser, R. Zafonte, M. H. Krengel, P. I. Martin, J. Frazier, M. R. Hamblin, J. A. Knight, W. P. Meehan, E. H. Baker, *J. Neurotrauma* **2014**, *31*, 1008.
[17] J. C. Rojas, F. Gonzalez-Lima, *Biochem. Pharmacol.* **2013**, *86*, 447.

[18] T. C. Wikramanayake, R. Rodriguez, S. Choudhary, L. M. Mauro, K. Nouri, L. A. Schachner, J. J. Jimenez, *Lasers Med. Sci.* **2012**, *27*, 431.
[19] M. R. Hamblin, S. T. Nelson, J. R. Strahan, *Photomed. Laser Surg.* **2018**, *36*, 241.
[20] H. Kobayashi, A. Furusawa, A. Rosenberg, P. L. Choyke, *Int. Immunol.* **2021**, *33*, 7.
[21] H. Monaco, S. Yokomizo, H. S. Choi, S. Kashiwagi, *View* **2022**, *3*, 20200110.
[22] M. V. P. de Sousa, in *Handbook of Low-Level Laser Therapy* (Eds: M. R. Hamblin, T. Agrawal, M. de Sousa), Pan Stanford Publishing Pte. Ltd, Sao Paolo **2017**.
[23] T. I. Karu, *Photochem. Photobiol.* **2008**, *84*, 1091.
[24] Y. Hatefi, *Annu. Rev. Biochem.* **1985**, *54*, 1015.
[25] W. Choi, K. Y. Baik, S. Jeong, S. Park, J. E. Kim, H. B. Kim, J. H. Chung, *Sci. Rep.* **2021**, *11*, 17329.
[26] P. L. V. Lima, C. V. Pereira, N. Nissanka, T. Arguello, G. Gavini, C. M. d. C. Maranduba, F. Diaz, C. T. Moraes, *J. Photochem. Photobiol. B* **2019**, *194*, 71.
[27] A. P. Sommer, M. K. Haddad, H.-J. Fecht, *Sci. Rep.* **2015**, *5*, 12029.
[28] J. E. Kim, Y. J. Woo, K. M. Sohn, K. H. Jeong, H. Kang, *Lasers Surg. Med.* **2017**, *49*, 940.
[29] A. R. N. Zamani, S. Saberianpour, M. H. Geranmayeh, F. Bani, L. Haghighi, R. Rahbarghazi, *Lasers Med. Sci.* **2020**, *35*, 299.
[30] V. Myrianthopoulos, K. Evangelou, P. V. S. Vasileiou, T. Cooks, T. P. Vassilakopoulos, G. A. Pangalis, M. Kouloukoussa, C. Kittas, A. G. Georgakilas, V. G. Gorgoulis, *Pharmacol. Ther.* **2019**, *193*, 31.
[31] P. Vasileiou, K. Evangelou, K. Vlasis, G. Fildisis, M. Panayiotidis, E. Chronopoulos, P.-G. Passias, M. Kouloukoussa, V. Gorgoulis, S. Havaki, *Cells* **2019**, *8*, 686.
[32] L. Hayflick, P. S. Moorhead, *Exp. Cell Res.* **1961**, *25*, 585.
[33] C. Quijano, L. Cao, M. M. Fergusson, H. Romero, J. Liu, S. Gutkind, I. I. Rovira, R. P. Mohney, E. D. Karoly, T. Finkel, *Cell Cycle* **2012**, *11*, 1383.
[34] V. Gorgoulis, P. D. Adams, A. Alimonti, D. C. Bennett, O. Bischof, C. Bishop, J. Campisi, M. Collado, K. Evangelou, G. Ferbeyre, J. Gil, E. Hara, V. Krizhanovsky, D. Jurk, A. B. Maier, M. Narita, L. Niedernhofer, J. F. Passos, P. D. Robbins, C. A. Schmitt, J. Sedivy, K. Vougas, T. von Zglinicki, D. Zhou, M. Serrano, M. Demaria, *Cell* **2019**, *179*, 813.
[35] S. He, N. E. Sharpless, *Cell* **2017**, *169*, 1000.
[36] M. Demaria, N. Ohtani, S. A. Youssef, F. Rodier, W. Toussaint, J. R. Mitchell, R.-M. Laberge, J. Vijg, H. Van Steeg, M. E. T. Dollé, J. H. J. Hoeijmakers, A. de Bruin, E. Hara, J. Campisi, *Dev. Cell* **2014**, *31*, 722.
[37] J.-I. Jun, L. F. Lau, *Nat. Cell Biol.* **2010**, *12*, 676.
[38] K.-H. Kim, C.-C. Chen, R. I. Monzon, L. F. Lau, *Mol. Cell. Biol.* **2013**, *33*, 2078.
[39] V. Krizhanovsky, M. Yon, R. A. Dickins, S. Hearn, J. Simon, C. Miething, H. Yee, L. Zender, S. W. Lowe, *Cell* **2008**, *134*, 657.
[40] J. Campisi, *Nat. Rev. Cancer* **2003**, *3*, 339.
[41] J. Campisi, F. d'Adda di Fagagna, *Nat. Rev. Mol. Cell Biol.* **2007**, *8*, 729.
[42] G. C. Williams, *Evolution* **1957**, *11*, 398.
[43] P. F. L. da Silva, M. Ogrodnik, O. Kucheryavenko, J. Glibert, S. Miwa, K. Cameron, A. Ishaq, G. Saretzki, S. Nagaraja-Grellscheid, G. Nelson, T. von Zglinicki, *Aging Cell* **2019**, *18*, e12848.
[44] D. McHugh, J. Gil, *J. Cell Biol.* **2018**, *217*, 65.
[45] C. von Kobbe, *Aging* **2019**, *11*, 12844.
[46] M. R. Hamblin, *Photochem. Photobiol.* **2018**, *94*, 199.
[47] B. D. Chang, E. V. Broude, M. Dokmanovic, H. Zhu, A. Ruth, Y. Xuan, E. S. Kandel, E. Lausch, K. Christov, I. B. Roninson, *Cancer Res.* **1999**, *59*, 3761.
[48] A. Hernandez-Segura, S. Brandenburg, M. Demaria, *JoVE* **2018**, *136*, 57782. https://doi.org/10.3791/57782
[49] G. P. Dimri, X. Lee, G. Basile, M. Acosta, G. Scott, C. Roskelley, E. E. Medrano, M. Linskens, I. Rubelj, O. Pereira-Smith, *Proc. Natl. Acad. Sci. U S A* **1995**, *92*, 9363.
[50] A. Hernandez-Segura, J. Nehme, M. Demaria, *Trends Cell Biol.* **2018**, *28*, 436.
[51] D. J. Kurz, S. Decary, Y. Hong, J. D. Erusalimsky, *J. Cell Sci.* **2000**, *113*, 3613.
[52] B. Y. Lee, J. A. Han, J. S. Im, A. Morrone, K. Johung, E. C. Goodwin, W. J. Kleijer, D. DiMaio, E. S. Hwang, *Aging Cell* **2006**, *5*, 187.
[53] W.-P. Hu, J.-J. Wang, C.-L. Yu, C.-C. E. Lan, G.-S. Chen, H.-S. Yu, *J. Invest. Dermatol.* **2007**, *127*, 2048.
[54] T. D. Magrini, N. V. dos Santos, M. P. Milazzotto, G. Cerchiaro, H. da Silva Martinho, *J. Biomed. Opt.* **2012**, *17*, 1015161.
[55] J. Kujawa, K. Pasternak, I. Zavodnik, R. Irzmański, D. Wróbel, M. Bryszewska, *Lasers Med. Sci.* **2014**, *29*, 1663.
[56] Y.-Y. Huang, S. K. Sharma, J. Carroll, M. R. Hamblin, *Dose-Response* **2011**, *9*, 602.
[57] A. P. Fernandez, M. d. A. Junqueira, N. C. T. Marques, M. A. A. M. Machado, C. F. Santos, T. M. Oliveira, V. T. Sakai, *J. Appl. Oral Sci.* **2016**, *24*, 332.
[58] M. Khadra, S. P. Lyngstadaas, H. R. Haanæs, K. Mustafa, *Biomaterials* **2005**, *26*, 3503.
[59] H.-S. Yu, C.-S. Wu, Y.-H. Kao, M.-H. Chiou, C.-L. Yu, *J. Invest. Dermatol.* **2003**, *120*, 56.
[60] H. Abrahamse, N. N. Houreld, S. Muller, L. Ndlovu, *Med. Technol. SA* **2010**, *24*, 8.
[61] J. A. de Villiers, N. N. Houreld, H. Abrahamse, *Stem Cell Rev. Rep.* **2011**, *7*, 869.
[62] K. Kim, J. Lee, H. Jang, S. Park, J. Na, J. Myung, M.-J. Kim, W.-S. Jang, S.-J. Lee, H. Kim, H. Myung, J. Kang, S. Shim, *Int. J. Mol. Sci.* **2019**, *20*, 1131.
[63] D. Gagnon, T. W. G. Gibson, A. Singh, A. R. zur Linden, J. E. Kazienko, J. LaMarre, *BMC Vet. Res.* **2016**, *12*, 73. https://doi.org/10.1186/s12917-016-0689-5
[64] L. Laakso, C. Richardson, T. Cramond, *J. Physiother.* **1993**, *39*, 95.
[65] A. Amaroli, C. Pasquale, A. Zekiy, S. Benedicenti, A. Marchegiani, M. G. Sabbieti, D. Agas, *J. Tissue Eng.* **2022**, *13*, 204173142211101.
[66] N. N. Pavlova, C. B. Thompson, *Cell Metab.* **2016**, *23*, 27.
[67] S. G. Menon, P. C. Goswami, *Oncogene* **2007**, *26*, 1101.
[68] M. Fallah, H. Mohammadi, F. Shaki, Z. Hosseini-Khah, M. Moloudizargari, A. Dashti, A. Ziar, A. Mohammadpour, A. Mirshafa, M. Modanloo, M. Shokrzadeh, *Life Sci.* **2019**, *232*, 116677.
[69] E. Rovillain, L. Mansfield, C. Caetano, M. Alvarez-Fernandez, O. L. Caballero, R. H. Medema, H. Hummerich, P. S. Jat, *Oncogene* **2011**, *30*, 2356.
[70] C. Correia-Melo, J. F. Passos, *Biochim. Biophys. Acta* **2015**, *1847*, 1373.
[71] A. Höhn, D. Weber, T. Jung, C. Ott, M. Hugo, B. Kochlik, R. Kehm, J. König, T. Grune, J. P. Castro, *Redox Biol.* **2017**, *11*, 482.

[72] J. F. Passos, G. Nelson, C. Wang, T. Richter, C. Simillion, C. J. Proctor, S. Miwa, S. Olijslagers, J. Hallinan, A. Wipat, G. Saretzki, K. L. Rudolph, T. B. L. Kirkwood, T. von Zglinicki, *Mol. Syst. Biol.* **2010**, *6*, 347.
[73] V. R. Baichwal, P. A. Baeuerle, *Curr. Biol.* **1997**, *7*, R94.
[74] T. Wang, X. Zhang, J. J. Li, *Int. Immunopharmacol.* **2002**, *2*, 1509.
[75] H. P. Kim, *Biomol. Ther.* **2014**, *22*, 491.
[76] J. M. Suski, M. Lebiedzinska, M. Bonora, P. Pinton, J. Duszynski, M. R. Wieckowski, *Methods Mol. Biol.* **2012**, *810*, 183.
[77] M. A. Aon, S. Cortassa, B. O'Rourke, *Biochim. Biophys. Acta* **2010**, *1797*, 865.
[78] S. S. Korshunov, V. P. Skulachev, A. A. Starkov, *FEBS Lett.* **1997**, *416*, 15.
[79] I. Golovynska, S. Golovynskyi, Y. V. Stepanov, L. V. Garmanchuk, L. I. Stepanova, J. Qu, T. Y. Ohulchanskyy, *J. Cell. Physiol.* **2019**, *234*, 15989.
[80] I. Golovynska, S. Golovynskyi, Y. V. Stepanov, L. I. Stepanova, J. Qu, T. Y. Ohulchanskyy, *J. Photochem. Photobiol. B* **2021**, *214*, 112088.
[81] A. Tani, F. Chellini, M. Giannelli, D. Nosi, S. Zecchi-Orlandini, C. Sassoli, *Int. J. Mol. Sci.* **2018**, *19*, 1946.
[82] A. Görlach, K. Bertram, S. Hudecova, O. Krizanova, *Redox Biol.* **2015**, *6*, 260.
[83] M. J. Berridge, *Biochem. Soc. Trans.* **2012**, *40*, 297.
[84] G. Szabadkai, M. R. Duchen, *Physiology* **2008**, *23*, 84.
[85] P. Vaupel, G. Multhoff, *J. Physiol.* **2021**, *599*, 1745.
[86] O. Warburg, *Science* **1956**, *1979*, 269.
[87] S. Srinivasan, M. Guha, D. W. Dong, K. A. Whelan, G. Ruthel, Y. Uchikado, S. Natsugoe, H. Nakagawa, N. G. Avadhani, *Oncogene* **2016**, *35*, 1585. https://doi.org/10.1038/onc.2015.227
[88] V. I. Korolchuk, S. Miwa, B. Carroll, T. von Zglinicki, *EBioMedicine* **2017**, *21*, 7.
[89] B. K. Singh, M. Tripathi, R. Sandireddy, K. Tikno, J. Zhou, P. M. Yen, *Aging* **2020**, *12*, 13958.
[90] C. M. Gonçalves de Faria, H. Ciol, V. Salvador Bagnato, S. Pratavieira, *Biomed. Opt. Express* **2021**, *12*, 3902.
[91] V. Aggarwal, H. S. Tuli, A. Varol, F. Thakral, M. B. Yerer, K. Sak, M. Varol, A. Jain, M. A. Khan, G. Sethi, *Biomolecules* **2019**, *9*, 735.
[92] B. Perillo, M. Di Donato, A. Pezone, E. Di Zazzo, P. Giovannelli, G. Galasso, G. Castoria, A. Migliaccio, *Exp. Mol. Med.* **2020**, *52*, 192.
[93] J. Cahu, B. Sola, *JoVE* **2013**, *78*, 50494. https://doi.org/10.3791/50494-v
[94] Thermo Fisher Scientific, CellEvent™ Senescence Green Flow Cytometry Assay Kit. Thermo Fisher Scientific Inc. **2019**. https://www.thermofisher.com/document-connect/document-connect.html?url=https://assets.thermofisher.com/TFS-Assets%2FLSG%2Fmanuals%2FMAN0018281_CellEvent_Senescence_Green_Flow_Cytometry_Assay_Kit_PIS.pdf (accessed: February 2023).

SUPPORTING INFORMATION

Additional supporting information can be found online in the Supporting Information section at the end of this article.

How to cite this article: I. Kalampouka, R. R. Mould, S. W. Botchway, A. M. Mackenzie, A. V. Nunn, E. L. Thomas, J. D. Bell, *J. Biophotonics* **2024**, e202400046. https://doi.org/10.1002/jbio.202400046